



Effects of using different exposure data to estimate changes in premature mortality attributable to PM_{2.5} and O₃ in China[☆]

Chunlu Wang^a, Yiyi Wang^a, Zhihao Shi^a, Jinjin Sun^a, Kangjia Gong^a, Jingyi Li^a, Momei Qin^a, Jing Wei^b, Tiantian Li^c, Haidong Kan^d, Jianlin Hu^{a,*}

^a Jiangsu Key Laboratory of Atmospheric Environment Monitoring and Pollution Control, Collaborative Innovation Center of Atmospheric Environment and Equipment Technology, Nanjing University of Information Science & Technology, Nanjing, 210044, China

^b Department of Atmospheric and Oceanic Science, Earth System Science Interdisciplinary Center, University of Maryland, College Park, MD, 20740, USA

^c National Institute of Environmental Health, Chinese Center for Disease Control and Prevention, Beijing, 100021, China

^d School of Public Health, Key Lab of Public Health Safety of the Ministry of Education, Fudan University, Shanghai, 200032, China



ARTICLE INFO

Keywords:

Monitoring data
Air quality model predictions
Satellite observations
Premature mortality
Population density

ABSTRACT

The assessment of premature mortality associated with the dramatic changes in fine particulate matter (PM_{2.5}) and ozone (O₃) has important scientific significance and provides valuable information for future emission control strategies. Exposure data are particularly vital but may cause great uncertainty in health burden assessments. This study, for the first time, used six methods to generate the concentration data of PM_{2.5} and O₃ in China between 2014 and 2018, and then quantified the changes in premature mortality due to PM_{2.5} and O₃ using the Environmental Benefits Mapping and Analysis Program-Community Edition (BenMAP-CE) model. The results show that PM_{2.5}-related premature mortality in China decreases by 263 (95% confidence interval (CI95): 142–159) to 308 (CI95: 213–241) thousands from 2014 to 2018 by using different concentration data, while O₃-related premature mortality increases by 67 (CI95: 26–104) to 103 (CI95: 40–163) thousands. The estimated mean changes are up to 40% different for the PM_{2.5}-related mortality, and up to 30% for the O₃-related mortality if different exposure data are chosen. The most significant difference due to the exposure data is found in the areas with a population density of around 10³ people/km², mostly located in Central China, for both PM_{2.5} and O₃. Our results demonstrate that the exposure data source significantly affects mortality estimations and should thus be carefully considered in health burden assessments.

1. Introduction

The threat of air pollution is a global health concern (Lelieveld et al., 2015). The global disease burden (GDB) studies have attributed about 2 million premature deaths every year to air pollution in China (Yin et al., 2020). Ground-level PM_{2.5} (particulate matter with an aerodynamic diameter equal to or less than 2.5 μm) and ozone (O₃) are the two major pollutants in China. To protect public health, the central government of China has made tremendous efforts to reduce coal use, eliminate low energy utilization, improve the vehicle standards, and install desulfurization and denitrification units, all of which have greatly improved air quality in China since 2013 (Chen et al., 2020; Zheng et al., 2017). Recent studies have shown that the concentration of PM_{2.5} in China dropped by 28% from 2014 to 2018 (Fan et al., 2020), and continues to

decrease by 0.62 μg/m³ every year in East China (Madaniyazi et al., 2015). In contrast, O₃ has shown an increasing trend in China, and annual mean O₃ concentrations were projected to increase to up to 95 μg/m³ by 2050 (Zhong et al., 2019).

The assessment of premature mortality associated with the dramatic changes in PM_{2.5} and O₃ has important scientific significance and provides valuable information for future emission control strategies. A few studies have tried to quantify the premature mortality associated with the apparent changes in PM_{2.5} and O₃ in China. For example, Silver et al. (2020) estimated that PM_{2.5}-related premature mortality is reduced by 150000 deaths per year from 2015 to 2017. Huang et al. (2018) reported that the premature mortality attributable to O₃ increased by about 77000 from 2013 to 2017. However, the assessment is subjected to high uncertainties associated with various parameters, one of which is the

[☆] This paper has been recommended for acceptance by Admir C. Targino.

* Corresponding author.

E-mail address: jianlinhu@nuist.edu.cn (J. Hu).

exposure data of PM_{2.5} and O₃. To obtain accurate population exposure over a large geographical area, several methods have been developed and evaluated using ambient monitoring data, satellite-derived data, air quality model (AQM) predictions, or hybrid methods by combining two or three of the above three types of data (Baxter et al., 2013; Brauer et al., 2016; Bravo et al., 2012; Kim et al., 2015; Oakes et al., 2014; Ozkaynak et al., 2013). These methods have been widely utilized in estimating the health burden of air pollution in China. Rohde and Muller (2015) attributed 1.6 million premature deaths to outdoor PM_{2.5} in 2014 using the monitoring PM_{2.5} data of the official Chinese air quality reporting system. Li et al. (2020) estimated 1.31 million premature mortality due to ambient PM_{2.5} in 2016 using predicted concentrations from the Weather Research and Forecasting model coupled with Chemistry (WRF-Chem). Liang et al. (2019) estimated 120000 all-cause mortality stemming from violations in the O₃ standards in China in 2016 using fused satellite and monitoring O₃ data. Wang et al. (2020b) estimated 186000 respiratory deaths per year were associated with O₃ exposures during 2013–2017 based on hybrid O₃ data of AQM predictions and monitoring observations. These studies have selected different exposure data, however, there are no relevant studies that compare systematically the differences in health risks due to different exposure data.

The choice of the exposure data source may create large uncertainties in the assessment of changes in PM_{2.5}- and O₃-related mortality. For example, Ding et al. (2019) estimated that the Air Pollution Prevention and Control Action Plan in China has reduced mortalities by 287000 from 2013 to 2017 using the PM_{2.5} predictions from the chemistry transport model combined with surface observation. In another study, the estimate was 176000 based on the satellite data (Xiao et al., 2021). Therefore, the effects of exposure data source on mortality assessments should be examined. However, such studies in China have yet to be reported in the literature.

In this study, we aimed to evaluate the difference in the assessment of the changes in PM_{2.5} and O₃ and their related mortality when choosing different sources of data in China, and to identify the causes of the difference. We characterized the spatiotemporal trends of PM_{2.5} and O₃ exposure in China with six commonly used methods (described in Section 2) and estimated the health burden associated with each exposure dataset.

2. Materials and methods

2.1. Exposure estimates

Six methods were used to estimate the PM_{2.5} and O₃ changes between 2014 and 2018, including two methods using ambient monitoring data with Voronoi Neighbor Averaging (VNA) interpolation (OBS1) and Kriging interpolation (OBS2), predictions from the Weather Research and Forecasting-Community Multiscale Air Quality (WRF-CMAQ) modeling system (PRE), satellite-based observations (SAT), and two hybrid data HYB1 and HYB2: HYB1 combined the model predictions and the ambient monitor observations, and HYB2 also included the satellite observations with HYB1.

2.1.1. Ambient monitoring data (OBS1 and OBS2)

The monitor data in 2014 and 2018 were obtained from the China National Environmental Monitoring Center (CNEMC). Data quality control and quality assurance followed those mentioned in the study by Wang et al. (2014). There were 961 and 1584 monitoring stations in 2014 and 2018, respectively. In order to obtain gridded observation data, OBS1 used the VNA method to interpolate air quality monitoring data. VNA interpolation method uses the inverse distance weighting (IDW) method (Ding et al., 2016; Wang et al., 2015). The equations are as follows:

$$Grid_E = \sum_{i=1}^n Weight_i \times C_i \quad (1)$$

$$Weight_i = \frac{\frac{1}{D_i^2}}{\sum_{i=1}^n \frac{1}{D_i^2}} \quad (2)$$

where $Grid_E$ is the concentration of grid E , n is the number of neighboring monitors within the maximum influence distance, $Weight_i$ is the square distance weight of monitor i , C_i is the observed concentration at monitor i , and D_i is the distance between grid E and monitor i . The maximum influence distance was taken as 500 km. Some grid cells were far away from any observation stations; therefore, these grid cells had no values (as shown in Figure S1) and were not included in the analyses. These grids were all located in western China, which has a tiny population, and thus did not affect the health burden results.

Another commonly used interpolation method, the Ordinary Kriging interpolation method, is used in OBS2. Ordinary Kriging is a linear estimation system suitable for any inherently stationary random field that satisfies the isotropy assumption (Rohde and Muller, 2015; Xie et al., 2018). The formula is as follows:

$$Grid_E = \sum_{i=1}^n \lambda_i \times C_i \quad (3)$$

where λ_i is the weight coefficient monitor i . Here, λ_i not only relies on distance but also on the spatial arrangement of monitors. By fitting the distance and semivariance between observation data, the semivariance can be calculated according to the distance of any point, and λ_i is the optimal coefficient of semivariance from an unknown point to all known points, which were obtained in ArcGIS.

2.1.2. AQM data (PRE)

The Community Multi-scale Air Quality (CMAQ) model was applied to simulate PM_{2.5} and O₃ concentrations in China in 2014 and 2018 with a grid resolution of 36 km × 36 km. This model has been used to provide PM_{2.5} and O₃ fields in several health effect studies (Hu et al., 2017a; Liu et al., 2020; Wang et al., 2019; Yang et al., 2020). A detailed description of the model is described in these studies and references therein, and therefore only a brief description is provided here. The CMAQ model used in this study is a modified version of CMAQv5.0.2 (<http://www.cmascenter.org/cmaq/>) with updated SOA formation pathways from isoprene photochemistry (Hu et al., 2017b) and updated heterogeneous formation of nitrate and sulfate (Hu et al., 2016). Anthropogenic air pollutant emissions and biogenic emissions used in the simulation were estimated using the Multi-resolution Emission Inventory of China (MEIC) and the Model of Emissions of Gases and Aerosols from Nature version 2.1 (MEGAN2.1). Model predictions have been extensively evaluated against surface monitoring data in 2013, and satisfactory model performance on surface PM_{2.5} and O₃ concentrations has been reported in a previous study (Hu et al., 2016). Details can be found there and a brief evaluation of the predicted PM_{2.5} and O₃ in 2014 and 2018 is illustrated in Figure S2 in the Supporting Information.

2.1.3. Satellite-derived data (SAT)

The satellite-derived data were based on the 'ChinaHighAirPollutants' (CHAP) dataset (Wei et al., 2020, 2021) for ground-level PM_{2.5} and O₃. The PM_{2.5} dataset (available at <https://doi.org/10.5281/zenodo.4660858>) was generated using a newly developed space-time extremely randomized trees (STET) model based on the newly released MODIS Collection 6 MAIAC 1 km AOD products, meteorological variables, emissions, and auxiliary data, and its spatial resolution is 1 km. The O₃ dataset (available at <https://doi.org/10.5281/zenodo.3988420>) was generated using the extended STET model from the OMI/Aura Total Column O₃ products, as well as meteorological variables, pollutant emissions, and other auxiliary data. The spatial

resolution of O_3 was 25 km. Both the PM_{2.5} and O_3 datasets have high accuracy with a cross-validation coefficient of determination ($CV-R^2$) of 0.90 and 0.84. The root-mean-square error (RMSE) of each dataset is low, 10.09 $\mu\text{g}/\text{m}^3$ for PM_{2.5} and 20.11 $\mu\text{g}/\text{m}^3$ for O_3 .

2.1.4. Hybrid data (HYB1 and HYB2)

In this study, we adopted two-hybrid methods to generate the hybrid datasets of HYB1 and HYB2. HYB1 combines the AQM data with the monitoring observation data, and HYB2 combines the AQM data, monitoring data, and the satellite-derived data. The difference between the observed and the predicted concentrations was used to correct the concentrations in the grids without monitors using the IDW method, following the method used by Chen et al. (2014). The equations are as follows:

$$HYB_E = Grid_E + \sum_{i=1}^n Weight_i \times \Delta X_i \quad (4)$$

$$\Delta X_E = C_i + Grid_i \quad (5)$$

where HYB_E is the hybrid concentration of grid E , and $Grid_E$ is the “simulated” concentration of grid E . $Grid_E$ is the CMAQ simulated concentration in HYB1 and is the average of the simulated and satellite-derived concentration in HYB2 following the method used in the Global Burden of Disease (2013) study (Brauer et al., 2016). C_i and $Grid_i$ represents the ambient observed and “simulated” concentration at monitor i , respectively.

2.2. Health burden assessment

The Environmental Benefits Mapping and Analysis Program Community Edition (BenMAP-CE) version 1.5 developed by the U.S. EPA (Sacks et al., 2018) was used in this study to estimate the premature mortality due to exposure to PM_{2.5} and O_3 in 2014 and 2018 respectively. Estimation of premature mortality in BenMAP-CE has two steps: the first step is to create an air quality surface as discussed in Section 2.1; the second step is to estimate the PM_{2.5} and O_3 -related premature mortality using the following equation:

$$M = y_0 P [(RR - 1) / RR] \quad (6)$$

where y_0 is the baseline mortality rate due to a particular disease category, including lung cancer (LC), chronic obstructive pulmonary disease (COPD), ischemic heart disease (IHD), and stroke. The baseline mortalities in 2014 and 2018 were obtained from the China Public Health and Family Planning Statistical Yearbook 2015, 2019 (CPHFSY, 2015&2019). P is the population. In this study, gridded population data were obtained from the LandScan™ database for 2014 (Bright et al., 2015) and 2018 (Rose et al., 2019). LandScan™ spatial resolution is at approximately 1 km (30'' × 30''), and the population raster data was converted to vector points and aggregated into 36 km × 36 km grid data to match the resolution of the WRF-CMAQ domain.

Relative risk (RR) refers to the ratio of the probability of an event occurring when a group of people are exposed to a certain risk and not exposed to that risk. The RR of LC, COPD, IHD, and stroke from long-term PM_{2.5} exposure was calculated using the integrated exposure-response (IER) function (Burnett et al., 2014):

$$RR(C) = 1 + \alpha \{1 - \exp[-\beta(C - C_{cf})^\delta]\} \quad (7)$$

where α , β , and δ are the exposure-response coefficients obtained from Hu et al. (2017a). C is the annual mean PM_{2.5} concentrations in units of $\mu\text{g}/\text{m}^3$, and C_{cf} (2.4 $\mu\text{g}/\text{m}^3$) is the threshold, below which it is assumed that there is no additional risk. The RR of O_3 exposure-related non-accidental mortality was calculated as:

$$RR = \exp^{\beta(C - C_{cf})} \quad (8)$$

where β is the coefficient between the concentration and non-accidental mortality and is obtained from Turner et al. (2015). C is the annual mean maximum daily 8-h average O_3 (O_3 -MDA8) concentrations in units of ppb and C_{cf} is the threshold, which is 26.7 ppb in this study.

3. Results

3.1. Concentration changes

Table 1 illustrates the annual mean concentrations of PM_{2.5} and O_3 -MDA8 in 2014 and 2018 as estimated by the six different methods. The concentrations represent annual mean over all of the study grids (shown in **Figure S1**). The estimated annual mean PM_{2.5} in 2014 ranges from 32.1 to 52.2 $\mu\text{g}/\text{m}^3$, generally falls in the range reported by Li et al. (2021) (36.1 $\mu\text{g}/\text{m}^3$) and Rohde et al. (Rohde and Muller, 2015) (52.0 $\mu\text{g}/\text{m}^3$) for this year. The concentration of annual mean PM_{2.5} is estimated to drop to 18.0–34.4 $\mu\text{g}/\text{m}^3$ in 2018. All six methods show a declining trend of PM_{2.5}, but the estimated PM_{2.5} levels are largely different. The PRE method predicts the lowest country-wide mean PM_{2.5} both in 2014 (32.1 $\mu\text{g}/\text{m}^3$) and 2018 (18.0 $\mu\text{g}/\text{m}^3$), whereas the observation-based methods (OBS1, OBS2, and SAT) generally yield higher PM_{2.5} estimates (about 50 $\mu\text{g}/\text{m}^3$ in 2014 and over 30 $\mu\text{g}/\text{m}^3$ in 2018). Not surprisingly, the hybrid methods (HYB1 and HYB2) yield the medium estimates for PM_{2.5} in 2014 and 2018. The PM_{2.5} reduction from 2014 to 2018 as estimated by PRE is 14.0 $\mu\text{g}/\text{m}^3$, which is close to that estimated by OBS1 (15.1 $\mu\text{g}/\text{m}^3$) and OBS2 (17.6 $\mu\text{g}/\text{m}^3$), but much less than the value estimated by SAT (20.8 $\mu\text{g}/\text{m}^3$). Furthermore, the hybrid methods yield the smallest PM_{2.5} changes (HYB1: 11.0 $\mu\text{g}/\text{m}^3$ and HYB2: 10.1 $\mu\text{g}/\text{m}^3$), which is similar to the result of Xiao et al. (2020) with satellite data (11.2–12.8 $\mu\text{g}/\text{m}^3$). Paired t-tests show that the differences between the methods for PM_{2.5} (also for O_3) are statistically significant with p values less than 0.01.

The country-wide annual mean O_3 -MDA8 concentrations in 2014 are estimated at 39.2–48.7 ppb, which are consistent with 42.5 ± 6.8 ppb (mean ± standard deviation) in a previous study (Lin et al., 2018). The estimates for O_3 -MDA8 in 2018 range from 43.0 to 51.8 ppb. All methods capture the O_3 increasing trend. In contrast to the results of PM_{2.5}, PRE generally produces the highest O_3 estimates in both 2014 and 2018, but it produces the lowest O_3 increase (3.1 ppb) among the six methods. The O_3 increase estimate between PRE and SAT (3.9 ppb) is close. OBS2 yields the highest O_3 increase (7.7 ppb), which is also much higher than OBS1 (4.7 ppb) despite the same observation data being used in the two methods.

Fig. 1 shows the spatial distribution of the changes in PM_{2.5} and O_3 -MDA8 concentrations between 2014 and 2018 (the spatial distributions of PM_{2.5} in 2014 and 2018 of the six data sources are shown in **Figure S3**, and those of O_3 -MDA8 are shown in **Figure S4**). A decrease trend in PM_{2.5} while an increase trend in O_3 can be found in most parts of China, as predicted from all six methods. All methods predict that PM_{2.5} in Sichuan, Heilongjiang, Jilin, Liaoning, Beijing, and Hebei provinces decreases more significantly, but the reduction degree is most obvious in the PRE scenario. Some spatial differences can also be identified among the six sources of data. For example, the PM_{2.5} concentrations in parts of Xinjiang and Inner Mongolia increase slightly in OBS1 and HYB1, whereas the concentrations decrease in PRE.

For O_3 , no matter which method is used, the increase is more obvious in Hebei, Beijing, Shanxi, Henan, and Anhui provinces, compared to the other provinces. The degree of O_3 increase in PRE is the smallest. Some spatial differences are also observed among the different sources of data. OBS1 predicts that O_3 decreases in Tibet and west part of Gansu, and SAT predicts O_3 decreases in Tibet, south part of Xinjiang, and most of Southern China provinces. However, the declining O_3 in these areas is not captured in OBS2 and PRE.

Table 1

$\text{PM}_{2.5}$ and $\text{O}_3\text{-MDA8}$ annual mean concentration and its changes in different data sources. C14 and C18 represent the annual mean concentration in 2014, 2018 respectively. ΔC equals to C18 minus C14, ΔPWC equals to the difference between 2014 and 2018 PWC. OBS1: the data obtained from monitoring data with VNA interpolation; OBS2: the data obtained from monitoring data with Kriging interpolation; PRE: the data obtained from CMAQ predictions; SAT: the data obtained from satellite-derived methods; HYB1: the data obtained from fused monitoring data and CMAQ data; HYB2: the data obtained from fused monitoring data, CMAQ data and satellite data.

Data Sources	$\text{PM}_{2.5}$ ($\mu\text{g}/\text{m}^3$)						O_3 (ppb)					
	C14	C18	ΔC	PWC14	PWC18	ΔPWC	C14	C18	ΔC	PWC14	PWC18	ΔPWC
OBS1	48.2	33.0	-15.1	59.2	41.4	-17.8	41.6	46.3	4.7	41.8	49.3	7.5
OBS2	52.1	34.4	-17.6	59.4	41.5	-20.9	39.2	46.9	7.7	40.7	49.0	8.2
PRE	32.1	18.0	-14.0	68.4	38.1	-30.3	48.7	51.8	3.1	49.0	53.8	4.8
SAT	52.2	31.4	-20.8	66.2	40.5	-25.7	39.2	43.0	3.9	42.2	47.8	5.6
HYB1	41.5	30.5	-11.0	61.7	40.8	-17.9	43.7	48.0	4.3	43.5	50.6	7.1
HYB2	41.1	30.9	-10.1	57.4	40.5	-16.9	41.0	45.8	4.7	42.3	49.8	7.5

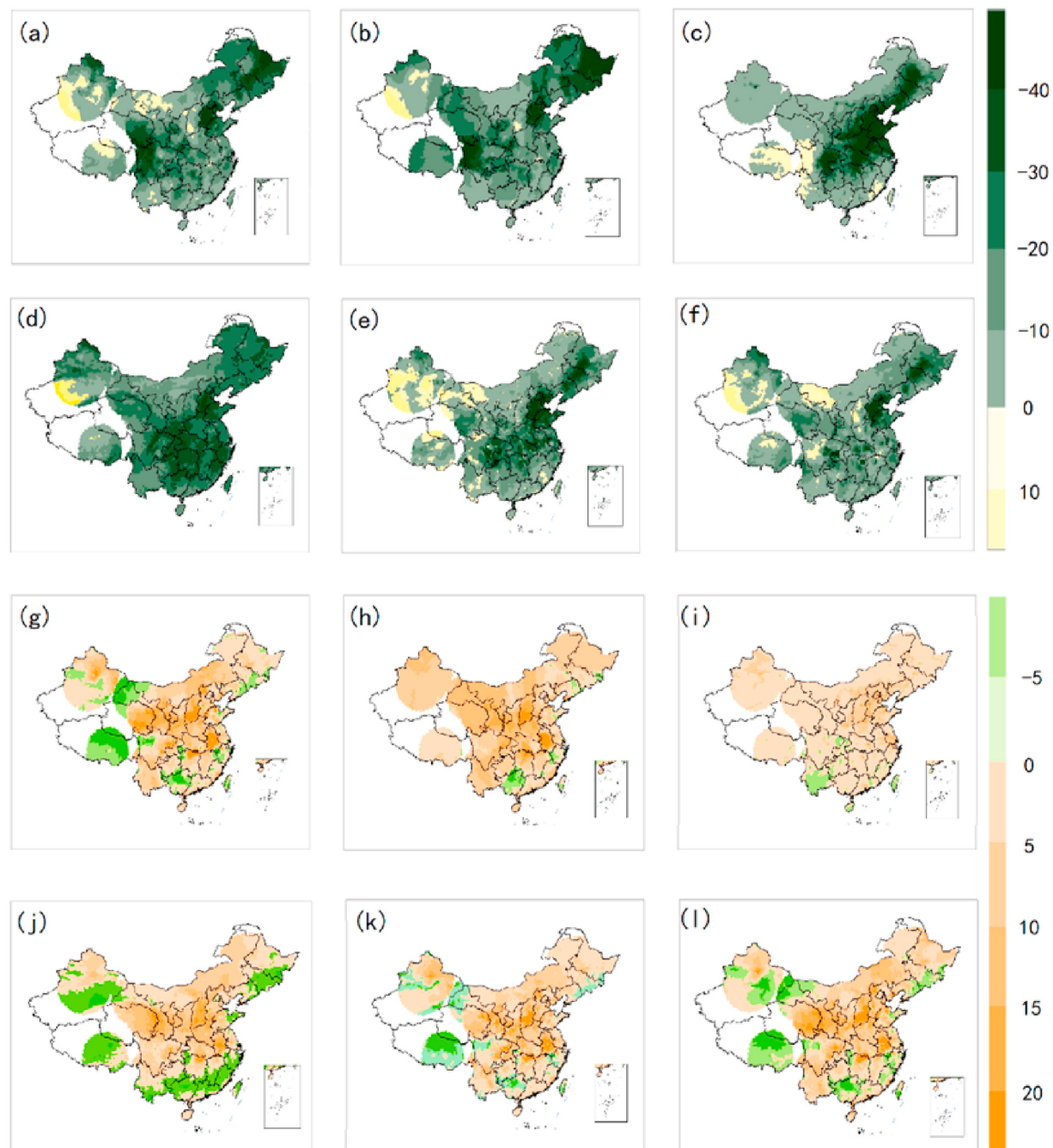


Fig. 1. The spatial distributions of $\text{PM}_{2.5}$ (unit: $\mu\text{g}/\text{m}^3$) (a–f) and $\text{O}_3\text{-MDA8}$ (unit: ppb) (g–l) annual mean concentration changes with OBS1 (a, g), OBS2 (b, h), PRE (c, i), SAT (d, j), HYB1 (e, k), HYB2(f, l).

3.2. Health burden changes

Table 2 illustrates the annual premature mortality changes due to changes in PM_{2.5} and O₃ between 2014 and 2018 in China. The PM_{2.5}-related premature mortalities vary from 1.38 (95% confidence intervals (CI95): 1.05–1.60) to 1.47 (CI95: 1.12–1.64) million in 2014 among the six methods. The numbers drop to 1.14 (CI95: 0.81–1.39) to 1.25 (CI95: 0.89–1.50) million in 2018. Therefore, PM_{2.5} improvement in China from 2014 to 2018 reduce premature mortality by 158 (CI95: 142–159) to 234 (CI95: 213–241) thousands. The PRE method estimates the largest health benefit whereas HYB2 estimates the lowest benefit. O₃-related premature mortality is estimated to be 0.16 (CI95: 0.06–0.26) to 0.25 (CI95: 0.09–0.39) million in 2014, and increase to 0.25 (CI95: 0.09–0.40) to 0.31 (CI95: 0.12–0.50) million in 2018 by the six methods. The number of O₃-related premature deaths increase by 67 (CI95: 26–104) to 103 (CI95: 40–163) thousands owing to O₃ increases.

Fig. 2 panels (a) to (f) show the spatial distribution of PM_{2.5}- and O₃-related mortality changes estimated with different methods. Most of the methods show that PM_{2.5}-related mortality is significantly reduced in the eastern and central regions of China. Although the spatial distributions are generally consistent, some differences among the methods can be observed in other regions. For example, OBS1, HYB1 and HYB2 show the PM_{2.5}-related mortality increases in part of Xinjiang, Tibet, and Inner Mongolia, whereas PRE shows slight PM_{2.5}-related mortality increases in part of Yunnan, Guangdong, and Fujian. It is worth noting that although the PM_{2.5} concentrations in Tibet decrease in PRE, the number of premature deaths in PRE remains unchanged. This is because the simulated annual mean concentration in Tibet in 2014 and 2018 is below the threshold.

Fig. 2 panels (g)–(l) show that O₃-related mortality increase significantly in Hebei, Shanxi, Henan, Anhui, and Beijing. Moreover, PRE and SAR estimate that O₃-related mortality has decreased in part of Yunnan whereas the other methods estimated an increasing trend. PRE estimates increases in O₃-related mortality in Guangxi, but all other methods estimate decreases. The SAT method also estimates that O₃-related mortality decreases in Guangdong, Fujian, and Zhejiang, which are not observed in OBS1, OBS2, and PRE.

Fig. 3 shows the estimated changes in PM_{2.5} and O₃ and their related mortality averaged by grid population density. OBS1 and OBS2 in PM_{2.5} concentration changes show small variations from less to more densely populated areas, whereas PRE and SAT exhibit a clear 'U' shape of variations with population density. Except for OBS2, all the other

methods reveal an increasing trend in the O₃ concentration changes with increasing population density. Because of the minor impact of less populated grids on mortality, the large difference in the mortality changes due to the different methods are mainly in the areas with a population density of around 10³ people/km² for both PM_{2.5} and O₃. Such areas are mostly located in Central China (**Figure S5**). This is due to the combined effect of population and concentration distributions. To illustrate this effect, we calculated the population-weighted concentrations (PWC), which is often used to characterize the overall population exposure levels. The results are shown in **Figure S6**. The most substantial difference in the changes in PWC among different data is found in Central China, due to the difference in the changes in PM_{2.5} and O₃ concentrations. Combined with large population in this region, the changes in mortality exhibit large discrepancy when choosing different exposure data.

4. Discussion

In this study, we estimated the changes in mortality associated with the changes in PM_{2.5} and O₃ between 2014 and 2018 in China with six exposure data derived from the most commonly used methods. Overall, we find that the estimated changes can be up to 40% different for the PM_{2.5}-related mortality and up to 30% for the O₃-related mortality if using different concentration data. The PM_{2.5}-related mortality change estimated by SAT is close to that by PRE, with a relative difference is within 5%. The O₃-related mortality changes estimated by SAT and OBS1 are very close. The hybrid methods have become more popular health burden studies. By combining different data, the hybrid methods generally yield the medium estimates.

Table 3 compares the changes in the PM_{2.5} and O₃ concentrations and their related premature mortalities during the recent years in China reported in previous studies and this study. The estimates in this study by different sources of data fall in the ranges reported in previous studies, both for PM_{2.5} and O₃, although the study years in these studies are slightly different. However, the difference in the estimates using different methods is obvious. The PM_{2.5} concentration reduction from 2014 to 2018 is 14.0–20.8 µg/m³. The maximum difference can be over 30%. The minimum reduction of 14.0 µg/m³ is estimated by PRE, and the maximum reduction of 20.8 µg/m³ is estimated by SAT. A similar difference is also found for the period of 2013–2017, during which Xiao et al. (2021) estimated of 18.0 µg/m³ PM_{2.5} reduction based on the satellite data, which is almost double that estimated by Ding et al. (2019) using the CMAQ predictions. The difference in the O₃ change estimates is even larger, ranging from 3.1 to 7.7 ppb (i.e., nearly 60% relative difference).

The difference in the estimated concentration changes does not necessarily correspond to the difference in the estimated mortality changes. The PRE method gives the lowest PM_{2.5} reduction, but the estimated avoided premature mortality is the highest among the six data sources. The similar finding is observed when comparing the work by Xiao et al. (2021) and Ding et al. (2019). The reason lies in the spatial distributions in the population and PM_{2.5} and O₃. The PWC results are illustrated in **Table 1**. For PM_{2.5}, the PWC values are all much greater than the average concentrations, indicating that more people reside in regions with higher PM_{2.5} concentrations. The PRE method yields the highest PWC in 2014, even though its estimation for the concentration is the lowest. The PM_{2.5} PWC in 2018 estimated by PRE is 2–3 µg/m³ lower than that produced by the other methods, even though the concentration is 12–16 µg/m³ lower. This is due to that the PRE method tends to well or slightly over-predict PM_{2.5} in the populous regions but largely under-predict PM_{2.5} in the remote, sparsely populated areas. As a result, the PRE method gives the largest changes in PM_{2.5} PWC, and leads to the greatest changes in the PM_{2.5}-related premature mortality. Interestingly, the average concentrations and PWC of O₃ are similar among all six data sources, suggesting O₃ is more spatially distributed than PM_{2.5}. PRE estimates the highest average O₃ concentrations but the least changes in

Table 2

PM_{2.5} and O₃-related premature mortality and its changes with different data sources from 2014 to 2018. M14 and M18 represent the premature mortality attributed to PM_{2.5} and O₃ in 2014, 2018 respectively. ΔM equals to M18 minus M14. The numbers in the parentheses represent 95% confidence intervals.

Data Sources	PM _{2.5} (Thousand)		O ₃ (Thousand)		ΔM	
	M14	M18	M14	M18		
OBS1	1403 (1047, 1638)	1236 (878, 1489)	−167 (−169, −149)	168 (64, 269)	261 (100, 417)	93 (36, 148)
	1412 (1058, 1646)	1249 (890, 1502)	−163 (−168, −144)	160 (61, 256)	263 (101, 419)	103 (40, 163)
	1378 (1049, 1604)	1144 (808, 1391)	−234 (−241, −213)	245 (94, 392)	312 (120, 496)	67 (26, 104)
PRE	1466 (1117, 1691)	1241 (880, 1496)	−225 (−237, −195)	179 (68, 286)	252 (97, 402)	73 (29, 116)
	1401 (1051, 1635)	1224 (868, 1478)	−177 (−183, −157)	186 (71, 298)	277 (106, 441)	91 (35, 143)
	1385 (1029, 1623)	1227 (870, 1481)	−158 (−159, −142)	173 (66, 277)	267 (102, 425)	94 (36, 148)

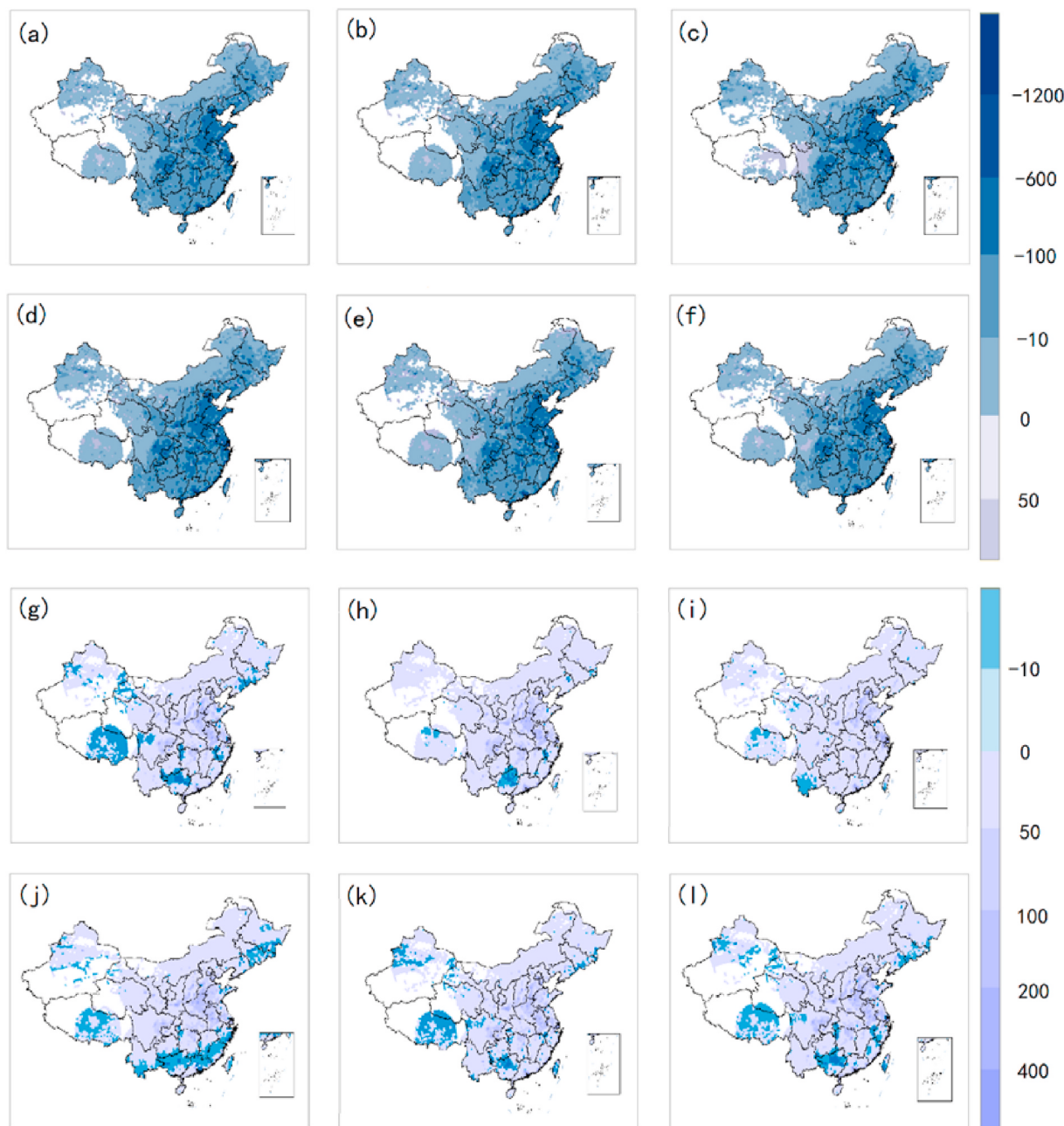


Fig. 2. The spatial distributions of PM_{2.5} (a–f) and O₃-related (g–l) premature mortality changes with OBS1 (a, g), OBS2 (b, h), PRE (c, i), SAT(d, j), HYB1 (e, k), HYB2(f, l). The unit is people.

O₃ PWC, leading to the lowest increase in the O₃-related premature mortality.

Overall, we suggest to use HYB2 for future health burden assessment. Each of the OBS, PRE and SAT methods has its own advantages and disadvantages. OBS accurately represents the exposure levels near the monitoring sites, but the spatial coverage is limited. PRE can provide concentrations over a large regional scale with high spatial and temporal resolutions, but its accuracy often affected by the model and the inputs data. SAT also can provide high resolution concentrations over a large region, but the data quality is affected by the satellite observations and the retrieval algorithms. By combining the different data, HYB2 data have the potential to improve the data quality by cutting down each other's shortages.

Assessment of premature mortalities is also affected by uncertainties in the exposure-response coefficients, population, and baseline

mortality rates. The uncertainties could be significant, as discussed in previous studies (Ding et al., 2019; Li et al., 2021; Wang et al., 2020b; Xie et al., 2018). These uncertainties also exist in our study, as indicated by the relatively large CI95 ranges. However, even with the same exposure-response coefficients, population and baseline mortality rate, we find that the differences in estimating the changes in premature mortality using different concentration data are significant enough so that one must be cautious when conducting air pollution-health effects studies. This is especially true for regions like Central China where the difference in estimated concentration changes in PM_{2.5} and O₃ is up to a factor of 3, and the difference in estimated mortality changes is up to a factor of 2. In addition to the data source, the parameter settings of models might also affect the magnitude of the difference. Comparing OBS1 and OBS2, even with the same observation data, the interpolation methods bring about a 2.5 µg/m³ (~15%) difference in estimating the

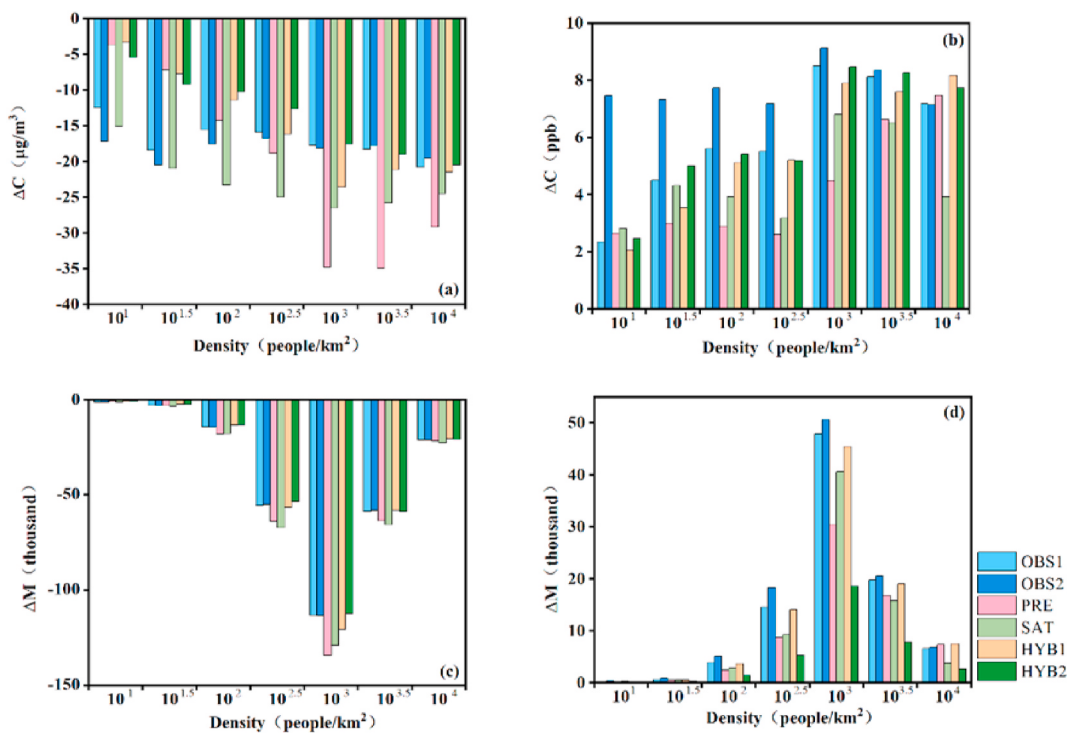


Fig. 3. (a) $\text{PM}_{2.5}$ and (b) O_3 -MDA8 annual mean concentration changes in different population density grids with different data sources; (c) $\text{PM}_{2.5}$ -related and (d) O_3 -related premature mortality changes in different population density grids with different data sources.

Table 3
Comparison of results in this study and previous studies.

region	year	exposure	Concentration change ($\mu\text{g}/\text{m}^3$ for $\text{PM}_{2.5}$ and ppb for O_3)	Mortality change (thousand)	References
$\text{PM}_{2.5}$	China	2013–2017	Satellite	-18.0	Xiao et al. (2021)
China	2013–2017	CMAQ	-9.0	Ding et al. (2019)	
China (74 key cities)	2013–2017	Monitors	-25.2	Huang et al. (2018)	
China	2015–2018	Monitors	-11.8	Wang et al. (2020a)	
China	2015–2019	Monitors	-12.9	Maji (2020)	
China	2014–2018	Monitors	-15.1 (OBS1) -17.6 (OBS2)	This study	
China	2014–2018	CMAQ	-14.0	This study	
China	2014–2018	Satellite	-20.8	This study	
China	2014–2018	Hybrid	-11.0 (HYB1) -10.1 (HYB2)	This study	
O_3	Eastern China	2012–2017	GEOS-Chem	8.9	Dang and Liao (2019)
China	2015–2017	WRF-chem	2.6	Silver et al. (2020)	
China	2013–2017	NAQPMS	5.5	Wang et al. (2020b)	
China (74 key cities)	2013–2017	Monitors	11.9	Huang et al. (2018)	
China	2015–2018	Monitors	6.4	Wang et al. (2020a)	
China	2014–2018	Monitors	4.7 (OBS1) 7.7 (OBS2)	This study	
China	2014–2018	CMAQ	3.1	This study	
China	2014–2018	Satellite	3.9	This study	
China	2014–2018	Hybrid	4.3 (HYB1) 4.7 (HYB2)	This study	

$\text{PM}_{2.5}$ changes, and 3.0 ppb (~40%) difference in estimating the O_3 changes. Grid resolution and model parameterizations on meteorology and chemistry may have some impacts on the PRE results. Liu et al. (2020) demonstrated that model resolution could lead to over 20% difference in premature mortality of O_3 . Nonetheless, the significant difference would have important impacts on designing future emission control plans. To resolve this issue, more observational and modeling studies should be conducted in this region to improve the assessment of population exposures and health impacts of air pollution.

5. Conclusions

Overall, our results demonstrate that exposure data derived from different methods can result in significant difference in estimating the premature mortality changes in China between 2014 and 2018. The estimated mean changes are up to 40% different for the $\text{PM}_{2.5}$ -related mortality, and up to 30% for the O_3 -related mortality. The most significant difference up to factor of 2 or 3 due to the exposure data is found in Central China for $\text{PM}_{2.5}$ and O_3 . To the best of our knowledge, this is the first effort to quantify the effects of the exposure data on estimating changes in premature mortalities due to $\text{PM}_{2.5}$ and O_3 changes in China.

by using six methods to generate the exposure data. Future studies are recommended to pay more attention in the areas like Central China to improve the assessment of population exposures and health impacts of air pollution.

Author contributions

J.H. and C.W. designed the research and developed the methodology; C.W., Y.W., Z.S., J.S., and K.G. carried out the data analysis and C.W. led the writing; J.H., J.L., and M.Q. provided supervision and acquired the funding; J.W. assisted in data collection; T.L. and H.K. discussed the results; all authors contributed significant comments and editing of the paper.

Declaration of competing interest

The authors declare that they have no known competing financial interests or personal relationships that could have appeared to influence the work reported in this paper.

Acknowledgments

This work was supported by the National Natural Science Foundation of China (41975162, 42021004, and 41705102). The satellite 'China-HighAirPollutants' (CHAP) dataset is available at <https://weijing-rs.git-hub.io/product.html>.

Appendix A. Supplementary data

Supplementary data to this article can be found online at <https://doi.org/10.1016/j.envpol.2021.117242>.

References

- Baxter, L.K., Dionisio, K.L., Burke, J., Sarnat, S.E., Sarnat, J.A., Hodas, N., Rich, D.Q., Turpin, B.J., Jones, R.R., Mannhardt, E., Kumar, N., Beavers, S.D., Ozkaynak, H., 2013. Exposure prediction approaches used in air pollution epidemiology studies: key findings and future recommendations. *J. Expo. Sci. Environ. Epidemiol.* 23, 654–659.
- Brauer, M., Freedman, G., Frostad, J., van Donkelaar, A., Martin, R.V., Dentener, F., Dingen, R.V., Estep, K., Amini, H., Apté, J.S., Balakrishnan, K., Barregard, L., Broday, D., Feigin, V., Ghosh, S., Hopke, P.K., Knibbs, L.D., Kokubo, Y., Liu, Y., Ma, S., Morawska, L., Sangrador, J.L.T., Shaddick, G., Anderson, H.R., Vos, T., Forouzanfar, M.H., Burnett, R.T., Cohen, A., 2016. Ambient air pollution exposure estimation for the global burden of disease 2013. *Environ. Sci. Technol.* 50, 79–88.
- Bravo, M.A., Fuentes, M., Zhang, Y., Burr, M.J., Bell, M.L., 2012. Comparison of exposure estimation methods for air pollutants: ambient monitoring data and regional air quality simulation. *Environ. Res.* 116, 1–10.
- Bright, E.A., Rose, A.N., Urban, M.L., 2015. LandScan 2014. Oak Ridge National Laboratory, Oak Ridge, TN, p. 2014.
- Burnett, R.T., Pope, C.A., Ezzati, M., Olives, C., Lim, S.S., Mehta, S., Shin, H.H., Singh, G., Hubbell, B., Brauer, M., Anderson, H.R., Smith, K.R., Balmes, J.R., Bruce, N.G., Kan, H., Laden, F., Prüss-Ustün, A., Turner, M.C., Gapstur, S.M., Diver, W.R., Cohen, A., 2014. An integrated risk function for estimating the global burden of disease attributable to ambient fine particulate matter exposure. *Environ. Health Perspect.* 122, 397–403.
- Chen, G., Li, J.Y., Ying, Q., Sherman, S., Perkins, N., Rajeshwari, S., Mendola, P., 2014. Evaluation of observation-fused regional air quality model results for population air pollution exposure estimation. *Sci. Total Environ.* 485, 563–574.
- Chen, L., Zhu, J., Liao, H., Yang, Y., Yue, X., 2020. Meteorological influences on PM2.5 and O3 trends and associated health burden since China's clean air actions. *Sci. Total Environ.* 744, 140837.
- Dang, R., Liao, H., 2019. Radiative forcing and health impact of Aerosols and ozone in China as the consequence of clean air actions over 2012–2017. *Geophys. Res. Lett.* 46, 12511–12519.
- Ding, D., Xing, J., Wang, S., Liu, K., Hao, J., 2019. Estimated contributions of emissions controls, meteorological factors, population growth, and changes in baseline mortality to reductions in ambient PM2.5 and pm2.5-related mortality in China, 2013–2017. *Environ. Health Perspect.* 127, 067009.
- Ding, D.A., Zhu, Y., Jang, C., Lin, C.J., Wang, S.X., Fu, J., Gao, J., Deng, S., Xie, J.P., Qiu, X.Z., 2016. Evaluation of health benefit using BenMAP-CE with an integrated scheme of model and monitor data during Guangzhou Asian Games. *J. Environ. Sci.* 42, 9–18.
- Fan, H., Zhao, C., Yang, Y., 2020. A comprehensive analysis of the spatio-temporal variation of urban air pollution in China during 2014–2018. *Atmos. Environ.* 220, 117066.
- Hu, J., Chen, J., Ying, Q., Zhang, H., 2016. One-year simulation of ozone and particulate matter in China using WRF/CMAQ modeling system. *Atmos. Chem. Phys.* 16, 10333–10350.
- Hu, J., Huang, L., Chen, M., Liao, H., Zhang, H., Wang, S., Zhang, Q., Ying, Q., 2017a. Premature mortality attributable to particulate matter in China: source contributions and responses to reductions. *Environ. Sci. Technol.* 51, 9950–9959.
- Hu, J., Wang, P., Ying, Q., Zhang, H., Chen, J., Ge, X., Li, X., Jiang, J., Wang, S., Zhang, J., Zhao, Y., Zhang, Y., 2017b. Modeling biogenic and anthropogenic secondary organic aerosol in China. *Atmos. Chem. Phys.* 17, 77–92.
- Huang, J., Pan, X., Guo, X., Li, G., 2018. Health impact of China's Air Pollution Prevention and Control Action Plan: an analysis of national air quality monitoring and mortality data. *The Lancet Planetary Health* 2, e313–e323.
- Kim, S.Y., Sheppard, L., Larson, T.V., Kaufman, J.D., Vedral, S., 2015. Combining PM2.5 component data from multiple sources: data consistency and characteristics relevant to epidemiological analyses of predicted long-term exposures. *Environ. Health Perspect.* 123, 651–658.
- Lelieveld, J., Evans, J.S., Fnais, M., Giannadaki, D., Pozzer, A., 2015. The contribution of outdoor air pollution sources to premature mortality on a global scale. *Nature* 525, 367.
- Li, Y., Liao, Q., Zhao, X., Tao, Y., Bai, Y., Peng, L., 2021. Premature mortality attributable to PM2.5 pollution in China during 2008–2016: underlying causes and responses to emission reductions. *Chemosphere* 263, 127925.
- Li, Y., Zhao, X., Liao, Q., Tao, Y., Bai, Y., 2020. Specific differences and responses to reductions for premature mortality attributable to ambient PM2.5 in China. *Sci. Total Environ.* 742, 140643.
- Liang, S., Li, X., Teng, Y., Fu, H., Chen, L., Mao, J., Zhang, H., Gao, S., Sun, Y., Ma, Z., Azzi, M., 2019. Estimation of health and economic benefits based on ozone exposure level with high spatial-temporal resolution by fusing satellite and station observations. *Environ. Pollut.* 255, 113267.
- Lin, Y., Jiang, F., Zhao, J., Zhu, G., He, X., Ma, X., Li, S., Sabel, C.E., Wang, H., 2018. Impacts of O3 on premature mortality and crop yield loss across China. *Atmos. Environ.* 194, 41–47.
- Liu, T., Wang, C., Wang, Y., Huang, L., Li, J., Xie, F., Zhang, J., Hu, J., 2020. Impacts of model resolution on predictions of air quality and associated health exposure in Nanjing, China. *Chemosphere* 249, 126515.
- Madanayazi, L., Nagashima, T., Guo, Y., Yu, W., Tong, S., 2015. Projecting fine particulate matter-related mortality in East China. *Environ. Sci. Technol.* 49, 11141–11150.
- Maji, K.J., 2020. Substantial changes in PM2.5 pollution and corresponding premature deaths across China during 2015–2019: a model prospective. *Sci. Total Environ.* 729, 138838.
- Oakes, M., Baxter, L., Long, T.C., 2014. Evaluating the application of multipollutant exposure metrics in air pollution health studies. *Environ. Int.* 69, 90–99.
- Ozkaynak, H., Baxter, L.K., Dionisio, K.L., Burke, J., 2013. Air pollution exposure prediction approaches used in air pollution epidemiology studies. *J. Expo. Sci. Environ. Epidemiol.* 23, 566–572.
- Rohde, R.A., Muller, R.A., 2015. Air pollution in China: mapping of concentrations and sources. *PLoS One*, e0135749.
- Rose, A.N., McKee, J.J., Urban, M.L., Bright, E.A., Sims, K.M., 2019. LandScan 2018. Oak Ridge National Laboratory, Oak Ridge, TN, p. 2018.
- Sacks, J.D., Lloyd, J.M., Zhu, Y., Anderton, J., Jang, C.J., Hubbell, B., Fann, N., 2018. The Environmental Benefits Mapping and Analysis Program – Community Edition (BenMAP-CE): a tool to estimate the health and economic benefits of reducing air pollution. *Environ. Model. Software* 104, 118–129.
- Silver, B., Conibeare, L., Reddington, C.L., Knote, C., Arnold, S.R., Spracklen, D.V., 2020. Pollutant emission reductions deliver decreased PM2.5-caused mortality across China during 2015–2017. *Atmos. Chem. Phys.* 20, 11683–11695.
- Turner, M., Jerrett, M., Pope, C., Krewski, D., Gapstur, S., Diver, W., Beckerman, B., Marshall, J., Su, J., Crouse, D., Burnett, R., 2015. Long-term ozone exposure and mortality in a large prospective study. *Am. J. Respir. Crit. Care Med.* 193.
- Wang, F., Qiu, X., Cao, J., Peng, L., Zhang, N., Yan, Y., Li, R., 2020a. Policy-driven Changes in the Health Risk of PM2.5 and O3 Exposure in China during 2013–2018. *Science of the Total Environment*, p. 143775.
- Wang, H., Zhu, Y., Jang, C., Lin, C.-J., Wang, S., Fu, J.S., Gao, J., Deng, S., Xie, J., Ding, D., Qiu, X., Long, S., 2015. Design and demonstration of a next-generation air quality attainment assessment system for PM2.5 and O3. *J. Environ. Sci.* 29, 178–188.
- Wang, Y., Wild, O., Chen, X., Wu, Q., Gao, M., Chen, H., Qi, Y., Wang, Z., 2020b. Health impacts of long-term ozone exposure in China over 2013–2017. *Environ. Int.* 144, 106030.
- Wang, Y., Ying, Q., Hu, J., Zhang, H., 2014. Spatial and temporal variations of six criteria air pollutants in 31 provincial capital cities in China during 2013–2014. *Environ. Int.* 73, 413–422.
- Wang, Y.Y., Shi, Z.H., Shen, F.Z., Sun, J.J., Huang, L., Zhang, H.L., Chen, C., Li, T.T., Hu, J.L., 2019. Associations of daily mortality with short-term exposure to PM2.5 and its constituents in Shanghai, China. *Chemosphere* 233, 879–887.
- Wei, J., Li, Z., Lyapustin, A., Sun, L., Peng, Y., Xue, W., Su, T., Cribb, M., 2021. Reconstructing 1-km-resolution high-quality PM2.5 data records from 2000 to 2018 in China: spatiotemporal variations and policy implications. *Rem. Sens. Environ.* 252, 112136.
- Wei, J., Li, Z.Q., Cribb, M., Huang, W., Xue, W.H., Sun, L., Guo, J.P., Peng, Y.R., Li, J., Lyapustin, A., Liu, L., Wu, H., Song, Y.M., 2020. Improved 1 km resolution PM2.5 estimates across China using enhanced space-time extremely randomized trees. *Atmos. Chem. Phys.* 20, 3273–3289.

- Xiao, Q., Geng, G., Liang, F., Wang, X., Lv, Z., Lei, Y., Huang, X., Zhang, Q., Liu, Y., He, K., 2020. Changes in spatial patterns of PM2.5 pollution in China 2000–2018: impact of clean air policies. *Environ. Int.* 141, 105776.
- Xiao, Q., Liang, F., Ning, M., Zhang, Q., Bi, J., He, K., Lei, Y., Liu, Y., 2021. The long-term trend of PM2.5-related mortality in China: the effects of source data selection. *Chemosphere* 263, 127894.
- Xie, Z., Qin, Y., Zhang, L., Zhang, R., 2018. Death effects assessment of PM2.5 pollution in China. *Pol. J. Environ. Stud.* 27, 1813–1821.
- Yang, J., Zhou, M., Li, M., Yin, P., Hu, J., Zhang, C., Wang, H., Liu, Q., Wang, B., 2020. Fine particulate matter constituents and cause-specific mortality in China: a nationwide modelling study. *Environ. Int.* 143, 105927.
- Yin, P., Brauer, M., Cohen, A.J., Wang, H., Li, J., Burnett, R.T., Stanaway, J.D., Causey, K., Larson, S., Godwin, W., Frostad, J., Marks, A., Wang, L., Zhou, M., Murray, C.J.L., 2020. The effect of air pollution on deaths, disease burden, and life expectancy across China and its provinces, 1990–2017: an analysis for the Global Burden of Disease Study 2017. *The Lancet Planetary Health* 4, e386–e398.
- Zheng, Y., Xue, T., Zhang, Q., Geng, G., Tong, D., Li, X., He, K., 2017. Air quality improvements and health benefits from China's clean air action since 2013. *Environ. Res. Lett.* 12, 114020.
- Zhong, M., Chen, F., Saikawa, E., 2019. Sensitivity of projected PM2.5- and O₃-related health impacts to model inputs: a case study in mainland China. *Environ. Int.* 123, 256–264.